Title

Long-Term Rate of Optic Disc Rim Loss in Glaucoma Patients Measured From Optic Disc Photographs With a Deep Neural Network.

Journal

Translational Vision Science & Technology, 13(9)

Authors

Jin, Sang
Bouris, Ella
Morales, Esteban
et al.

Publication Date

2024-09-03

DOI

10.1167/tvst.13.9.9

Peer reviewed

tvst

Artificial Intelligence

Long-Term Rate of Optic Disc Rim Loss in Glaucoma Patients Measured From Optic Disc Photographs With a Deep Neural Network

Sang Wook Jin[1,2], Ella Bouris[1], Esteban Morales[1], and Joseph Caprioli[3]

[1] Glaucoma Division, Stein Eye Institute, Los Angeles, CA, USA
[2] Department of Ophthalmology, Dong-A University College of Medicine, Busan, Republic of Korea
[3] Glaucoma Division, Stein Eye Institute, David Geffen School of Medicine, University of California at Los Angeles (UCLA), Los Angeles, CA, USA

Correspondence: Joseph Caprioli, Ophthalmology, Jules Stein Eye Institute, 100 Stein Plaza, Jules Stein Building, Los Angeles, CA 90095, USA. e-mail: caprioli@jsei.ucla.edu

Received: October 9, 2023
Accepted: August 9, 2024
Published: September 5, 2024

Keywords: glaucoma; artificial intelligence; optic disc; optic nerve; optic disc photography

Citation: Jin SW, Bouris E, Morales E, Caprioli J. Long-term rate of optic disc rim loss in glaucoma patients measured from optic disc photographs with a deep neural network. Transl Vis Sci Technol. 2024;13(9):9, https://doi.org/10.1167/tvst.13.9.9

Purpose: This study uses deep neural network–generated rim-to-disc area ratio (RADAR) measurements and the disc damage likelihood scale (DDLS) to measure the rate of optic disc rim loss in a large cohort of glaucoma patients.

Methods: A deep neural network was used to calculate RADAR and DDLS for each optic disc photograph (ODP). Patient demographics, diagnosis, intraocular pressure (IOP), and mean deviation (MD) from perimetry were analyzed as risk factors for faster progression of RADAR. Receiver operating characteristic (ROC) curves were used to compare RADAR and DDLS in their utility to distinguish glaucoma from glaucoma suspect (GS) and for detecting glaucoma progression.

Results: A total of 13,679 ODPs with evidence of glaucomatous optic nerve damage from 4106 eyes of 2407 patients with glaucoma or GS were included. Of these eyes, 3264 (79.5%) had a diagnosis of glaucoma, and 842 (20.5%) eyes were GS. Mean $\pm$ SD baseline RADAR of GS and glaucoma were 0.67 $\pm$ 0.13 and 0.57 $\pm$ 0.18, respectively ($P < 0.001$). Older age, greater IOP fluctuation, baseline MD, right eye, and diagnosis of secondary open-angle glaucoma were associated with slope of RADAR. The mean baseline DDLS of GS and glaucoma were 3.78 and 4.39, respectively. Both RADAR and DDLS showed a less steep slope in advanced glaucoma. In glaucoma, the change of RADAR and DDLS correlated with the corresponding change in MD. RADAR and DDLS had a similar ability to discriminate glaucoma from GS and detect disease progression. Area under the ROC curve of RADAR and DDLS was 0.658 and 0.648.

Conclusions: Automated calculation of RADAR and DDLS with a neural network can be used to evaluate the extent and long-term rate of optic disc rim loss and is further evidence of long-term nerve fiber loss in treated patients with glaucoma.

Translational Relevance: Our study provides a large clinic-based experience for RADAR and DDLS measurements in GS and glaucoma with a neural network.

Introduction

Glaucoma is a chronic, progressive optic neuropathy defined by the presence of characteristic patterns of damage to the optic nerve head (ONH) and typical visual field loss.[1] In general, clinically detectable structural changes precede perimetrically measured functional defects, and thus it is important to identify early structural changes associated with retinal ganglion cell loss. The rapid and accurate evaluation of structural changes and measurement of progression rate in the ONH plays a very important role in the diagnosis and management of patients with glaucoma.[2,3] Knowing the rate of glaucoma progression is essential to our long-term goal of preservation of vision in glaucoma patients. The ability to differentiate fast progressors from slow

progressors would direct appropriately aggressive treatment to those who are at highest risk for visual disability.[4]

Optic disc photography (ODP), scanning laser polarimetry, confocal scanning laser ophthalmoscopy, optical coherence tomography (OCT), and other techniques have been used for the evaluation of structural changes in glaucoma.[5,6] Compared with other imaging modalities, ODPs are relatively low-cost, easy to acquire, and widely accessible, and they have stable, standard platforms.[6–8] They have been collected for decades without essential changes in technology that might otherwise make them noncomparable over time. However, the interpretation of ODPs is subjective, and poor agreement among examiners and low reproducibility have been reported as major disadvantages.[6,9] ODPs would benefit from more standardized metrics for interpreting the extent of glaucomatous structural damage. Several such metrics have been used with some success. The most common, cup-to-disc ratio (CDR), is a traditional parameter for the detection of glaucoma and is a predictor of glaucoma progression.[10–12] However, CDR has significant limitations; CDR does not account for optic disc size; a small cup in a small optic disc can be associated with advanced glaucomatous damage, while a large cup in a large optic disc can be entirely normal. Therefore, CDR is less reliable for evaluating small or large optic discs.[13] Additionally, CDR is insensitive to focal disc rim changes.[14–16] For this reason, the disc damage likelihood scale (DDLS) was developed by Spaeth to minimize the issues of rim configuration and disc size,[17,18] although it may not be sensitive to small (intraclass) changes, and grading is subjective.[19] The rim to disc area ratio (RADAR) is a metric representing the entire rim area and as such can partly compensate for the limitations of CDR and DDLS but again may not be sensitive to small but significant focal areas of rim loss.[15–21]

Recently, we reported a deep neural network pipeline for automated identification of the optic disc rim and calculation of optic disc size.[22,23] This approach demonstrated acceptably accurate, objective, and highly reproducible rim segmentation and optic disc size estimates. The automated calculation of RADAR and DDLS can compensate for some of the limitations of conventionally used metrics for evaluating structural optic disc damage.[17,18,22–24] The present study uses deep neural network–generated RADAR measurements and DDLS gradings to measure the long-term rate of optic disc rim loss in a large cohort of glaucoma patients.

Methods

Participants

This retrospective study was conducted at the Stein Eye Institute of the University of California, Los Angeles (UCLA); adheres to the tenets of the Declaration of Helsinki; was approved by the UCLA Human Research Protection Program; and conforms to Health Insurance Portability and Accountability Act policies.

ODPs were taken from the UCLA Stein Eye Glaucoma database. Detailed inclusion and exclusion criteria about enrolled images can be found in the previously published studies.[20,21] Briefly, eligible patients met the following criteria: (1) clinical diagnosis of glaucoma or glaucoma suspect (GS), (2) age $\geq$18 years, (3) at least two ODPs, and (4) at least 2 years of follow-up. The exclusion criteria were any other causes for optic nerve or retinal abnormalities potentially affecting structural or functional status, including but not limited to proliferative diabetic retinopathy, central retinal vein occlusion, retinal detachment, and exudative age-related macular degeneration.

The diagnosis of glaucoma was based on a detailed review of paper charts (prior to 2013) and electronic medical records (after 2013). Eyes were classified as glaucomatous if they had, on ophthalmoscopic exam or ODPs, a glaucomatous optic disc (asymmetry of the disc rim width between the two eyes, focal or generalized neuroretinal rim thinning, notching, or characteristic retinal nerve fiber layer (RNFL) defects typical of glaucoma) and at least two consecutive abnormal visual field (VF) tests. An abnormal VF was defined as three or more nonedge points in the pattern deviation plot (with locations typical for glaucoma), with sensitivities below the 5th percentile and one of these points below the 1st percentile in a reliably performed field, a corrected pattern standard deviation with $P < 0.05$, and a Glaucoma Hemifield Test result outside normal limits. The GS cohort included patients with preglaucoma, ocular hypertension, anatomic narrow angle, and primary angle closure without glaucoma damage. Preglaucoma patients were defined as having a suspicious appearance of the optic nerve based on ODPs but normal VF results on at least two of their baseline visits. Ocular hypertension included patients who had a history of elevated intraocular pressure (IOP) over 21 mm Hg and had no glaucomatous damage on the optic disc, retinal nerve fiber layer, or visual field.

Patient demographics, diagnosis, IOP, RADAR, DDLS, and mean deviation (MD) values from visual fields were analyzed.

Ophthalmic Examinations

A deep neural network was used to calculate the optic disc size and automate the optic disc rim segmentation and output RADAR and DDLS for each ODP.[20,21] The progression rate of RADAR and DDLS was defined as the slope of RADAR and DDLS, respectively.

IOP fluctuation was defined as the standard deviation (SD) of IOP measurements while peak IOP was the highest single measurement.

Visual fields were performed with Humphrey Field Analyzer's Swedish Interactive Thresholding Algorithm Standard 24-2 strategy and a size III white stimulus (Carl Zeiss Meditec, Dublin, CA, USA). Reliable exams were defined as those with false-positive rates of 30% or less and fixation loss rates of 15% or less. Progression of visual field damage was defined as a significant ($P < 0.05$) MD rate of change of −0.5 dB/y or less.[25]

Patient Subgroups

Glaucoma patients were partitioned into primary open-angle glaucoma (POAG), primary angle closure glaucoma (PACG), and secondary open-angle glaucoma (SOAG) based on the diagnosis made by clinicians at baseline. SOAG included exfoliative glaucoma, pigmentary glaucoma, uveitic glaucoma, and steroid induced glaucoma. In addition, the glaucoma patients were divided into subgroups based on MD values according to the Anderson–Patella classification[26] into early-stage glaucoma with MD > −6 decibels (dB), moderate stage glaucoma with −6 ≥ MD > −12 dB, and advanced-stage glaucoma with MD ≤ −12 dB.

Statistical Analysis

Statistical analyses were performed with R statistical software (version 4.2.2; R Project for Statistical Computing, Vienna, Austria). The Shapiro test or the Kolmogorov–Smirnov test was used to test for normality. Mean and SD were used for normally distributed variables and median and interquartile range were used for nonnormally distributed variables. Categorical variables were analyzed by the χ^2 test or the Fisher exact test. Student's *t*-test or the Mann–Whitney *U* test was used for the analysis of continuous variables. Linear regression of RADAR and DDLS was used to measure the rates of rim loss. Differences regarding summary IOP measures and slope of RADAR were compared among different types of glaucoma with one-way analysis of variance with post hoc multiple comparisons. For comparison of the diagnostic ability to separate glaucoma from GS and the ability to detect progression of glaucoma between RADAR and DDLS, receiver operating characteristic (ROC) curves were built and the area under the ROC curve (AUC) was calculated. Pairwise comparisons of AUC were performed between RADAR and DDLS. *P* values less than 0.05 were used to indicate statistical significance.

Binomial logistic mixed-model analysis was performed on eyes with four or more fundus images to investigate which factors were associated with negative RADAR slope. Risk factors with $P < 0.2$ between eyes with negative RADAR slopes and others were then selected in the multivariable logistic mixed model. Random effect based on patient was applied to account for within-patient correlations due to the inclusion of both eyes.

Results

A total of 13,679 ODPs with evidence of glaucomatous optic nerve damage from 4106 eyes of 2407 patients with glaucoma or suspected glaucoma were included. Of these eyes, 3264 (79.5%) eyes had a diagnosis of glaucoma and 842 (20.5%) eyes were GS. Table 1 represents the baseline demographics and clinical characteristics of each group. The mean ± SD baseline RADAR in the glaucoma and GS groups were 0.57 ± 0.18 and 0.67 ± 0.13, respectively ($P < 0.001$). The mean ± SD baseline DDLS in the glaucoma and GS groups were 4.39 ± 1.23 and 3.78 ± 0.95, respectively ($P = 1.000$).

The frequency distribution according to glaucoma diagnosis is presented in Table 2. The majority of patients had a diagnosis of POAG (2969, 72.3%) followed by GS (842, 20.5%), SOAG (164, 4.0%), and PACG (131, 3.2%).

Figure 1 shows RADAR change over the entire follow-up time. RADAR decreased at a rate of –0.010 per year, and there was a statistically significant difference between baseline RADAR and final RADAR ($P < 0.001$). For GS patients, there was also a statistically significant difference between baseline RADAR and final RADAR ($P < 0.001$), and the decreasing rate of RADAR was –0.008 per year.

The baseline and slope of RADAR according to stage of glaucoma is shown in Table 3. There was a statistically significant difference in baseline RADAR between GS, early, moderate, and advanced glaucoma (Fig. 2). Eyes with GS and advanced glaucoma progressed significantly slower (defined by slope of RADAR) than eyes with early and moderate glaucoma.

Table 1. Demographics

Variables	Glaucoma $n = 1906$ (3264 Eyes)	GS $n = 501$ (842 Eyes)
Age (IQR, range), y	65.1 (14.6, 18.2 to 100)	61.0 (15.4, 18.1 to 89.2)
Sex, female, *n* (%)	1104 (58.0)	328 (65.5)
Follow-up (IQR, range), y	5.0 (8.4, 2.0 to 21.7)	4.1 (5.5, 2.0 to 21.1)
IOP, mean ± SD, mm Hg	14.2 ± 3.21	15.1 ± 3.20
IOP, *n* (IQR, range)	13.0 (17.0, 1.0 to 141.0)	7.0 (9.0, 1.0 to 96.0)
Baseline RADAR, mean ± SD	0.57 ± 0.18	0.67 ± 0.13
Final RADAR, mean ± SD	0.49 ± 0.19	0.62 ± 0.15
Baseline DDLS, mean ± SD	4.39 ± 1.23	3.78 ± 0.95
Final DDLS, mean ± SD	4.98 ± 1.47	4.11 ± 1.12
Baseline MD (IQR, range), dB	−1.93 (4.36, −28.12 to 3.16)	−0.72 (2.43, −27.45 to 3.66)
Final MD (IQR, range), dB	−2.64 (6.35, −29.03 to 8.96)	−0.45 (2.68, −25.41 to 4.95)
Race, *n* (%)		
Caucasian	1088 (57.1)	271 (54.1)
Asian	259 (13.6)	67 (13.4)
Black or African American	163 (8.6)	30 (6.0)
Hispanic	139 (7.3)	28 (5.6)
Others	257 (13.5)	105 (20.1)

IQR, interquartile range.

Table 2. Frequency Distribution According to Glaucoma Diagnosis

Diagnosis	Number (%) of Eyes
POAG	2969 (72.3)
PACG	131 (3.2)
SOAG	164 (4.0)
Exfoliative glaucoma	98 (2.4)
Pigmentary glaucoma	56 (1.4)
Steroid-induced glaucoma	10 (0.2)
GS	842 (20.5)
Preglaucoma	477 (11.6)
Anatomic narrow angle	265 (6.5)
Primary angle closure without glaucoma damage	5 (0.1)
Ocular hypertension	95 (2.3)

The baseline RADAR, slope of RADAR, and characteristics of IOP according to type of glaucoma are shown in Table 4. Baseline RADAR in POAG, PACG, and SOAG was significantly lower than in GS (Fig. 2). When comparing baseline RADAR of POAG, PACG, and SOAG, the baseline RADAR in POAG was significantly lower than in PACG (Fig. 3). RADAR in SOAG progressed significantly faster than GS, POAG, and PACG ($P < 0.001$). In addition, SOAG had higher peak IOP and SD of IOP than GS, POAG, and PACG (peak IOP: $P < 0.001$; SD of IOP: $P < 0.001$).

The results of the multivariable linear regression analyses for identifying the risk factors for progression of RADAR are shown in Table 5. In total, 1477 eyes (left eyes: 651, 44.1%; right eyes: 826, 55.9%) were included in the risk factor analysis. Older age ($P < 0.001$), higher SD of IOP ($P < 0.001$), baseline MD ($P < 0.001$), right eye ($P = 0.002$), and diagnosis of SOAG ($P = 0.021$) were associated with a negative RADAR slope.

The baseline and slope of DDLS according to stage of glaucoma are shown in Table 6. There was a statistically significant difference in baseline DDLS between GS, early, moderate, and advanced glaucoma ($P < 0.001$) (Fig. 4). In the post hoc multiple-comparison (Scheffé method) results of the slope of DDLS, there was a statistically significant difference between moderate and advanced glaucoma ($P = 0.007$).

The baseline and slope of DDLS according to type of glaucoma are shown in Table 7. A comparison of the baseline DDLS among GS, POAG, PACG, and SOAG can be found in Figure 5. There was no significant difference in the slope of the DDLS between any of the groups (GS and POAG: $P = 0.566$; GS and PACG: $P = 0.854$; GS and SOAG: $P = 0.355$; POAG and PACG: $P = 0.946$; POAG and SOAG: $P = 0.505$; PACG and SOAG: $P = 0.605$).

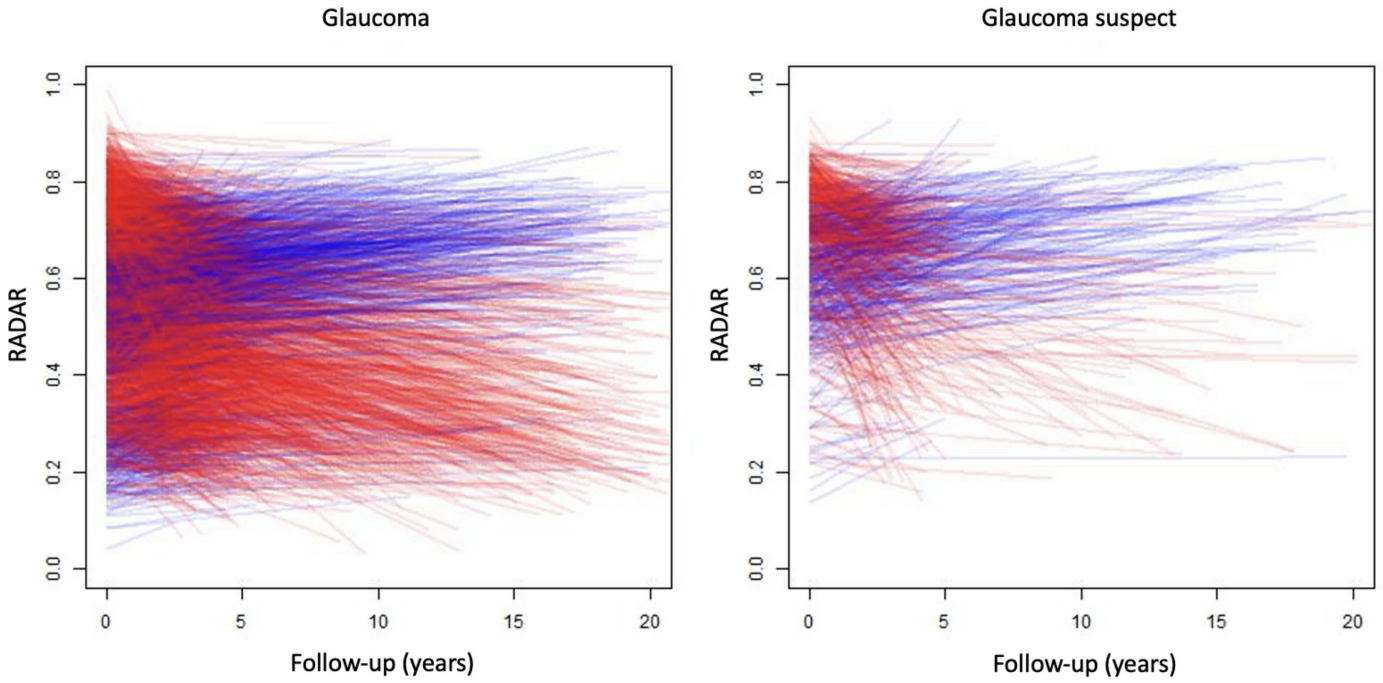

Figure 1. Change of rim to disc area ratio over follow-up time. *Blue line*: positive regression. *Red line*: negative regression.

Correlation between change in RADAR (final RADAR – baseline RADAR) and change in MD is shown in Figure 6. For glaucoma patients, the overall difference in RADAR significantly correlated with the difference in MD, although the relationship was weak ($R^2 = 0.03$, $P < 0.001$). In subgroup analyses, the difference in RADAR significantly correlated with difference in MD in each type of glaucoma except SOAG (POAG: $R^2 = 0.03$, $P < 0.001$; PACG: $R^2 = 0.09$, $P < 0.001$; SOAG: $R^2 = 0.01$, $P = 0.297$).

Figure 7 displays the correlation between the difference in DDLS (final – baseline) and the difference in MD (final – baseline). For glaucoma patients, the difference in DDLS significantly correlated with the difference in MD ($R^2 = 0.03$, $P < 0.001$). In subgroup analyses, the difference in DDLS significantly correlated with difference in MD in each type of glaucoma (POAG: $R^2 = 0.03$, $P < 0.001$; PACG: $R^2 = 0.11$, $P < 0.001$; SOAG: $R^2 = 0.03$, $P = 0.039$).

Figure 8 shows ROC curves for RADAR and DDLS for GS and glaucoma. AUCs of RADAR and DDLS were 0.69 and 0.67, respectively. The optimal cutoff values of RADAR and DDLS to distinguish between GS and glaucoma were 0.602 and 5, respectively. There was a statistically significant difference in AUC between RADAR and DDLS ($P = 0.03$).

Figure 9 shows the comparison between the ability of the slope of RADAR and DDLS to predict glaucoma progression at early and moderate stages of glaucoma. To reduce the floor effect of structural glaucomatous change, we removed eyes with VF baseline MD ≤ -12 dB.[27] The slopes of RADAR (AUC = 0.60) and DDLS (AUC = 0.59) were both able to discriminate progression of glaucoma from no progression in early- to moderate-stage glaucoma, with no statistically significant differences between the two ($P = 0.50$).

Table 3. Baseline RADAR and Slope of RADAR According to Stage of Glaucoma

Characteristic	GS	Early	Moderate	Advanced
Number (%) of eyes	842	2607 (79.9[a])	409 (12.5[a])	248 (7.6[a])
Baseline RADAR	0.67 ± 0.13	0.60 ± 0.16	0.46 ± 0.17	0.37 ± 0.16
Slope of RADAR	−0.008 ± 0.032	−0.011 ± 0.029	−0.007 ± 0.031	−0.007 ± 0.032

Values are presented as the mean ± SD unless otherwise indicated.
[a]Proportion of all glaucoma patients.

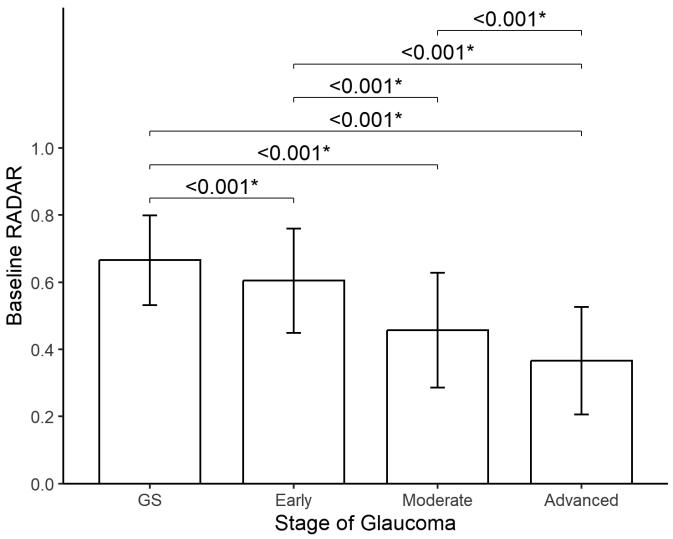

Figure 2. Comparison of baseline rim to disc area ratio according to stage of glaucoma. Early = early-stage glaucoma; moderate = moderate-stage glaucoma; advanced = advanced-stage glaucoma. *Statistical significance by one-way analysis of variance with post hoc multiple comparison (Scheffé method).

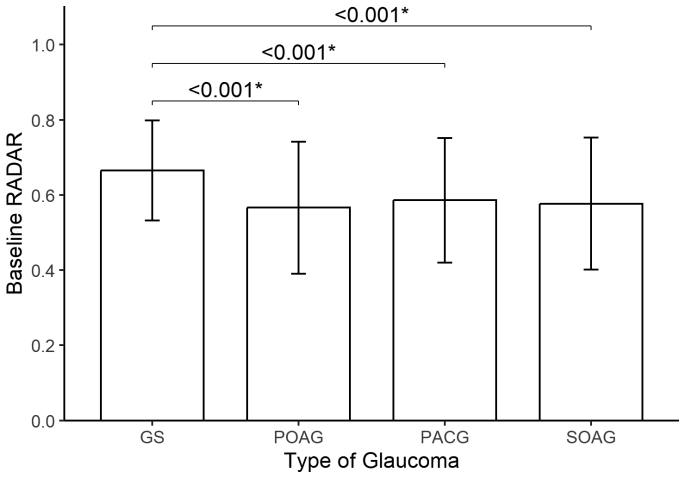

Figure 3. Comparison of baseline rim to disc area ratio according to type of glaucoma. *Statistical significance by one-way analysis of variance with post hoc multiple comparison (Scheffé method).

Discussion

Several metrics have been used to quantify the extent of structural glaucomatous optic disc damage from ODPs. Conventionally, CDR has been used for glaucoma diagnosis and determination of glaucoma progression.[10–12] However, because of the previously discussed limitations of CDR, an alternative parameter for the evaluation of glaucomatous optic nerve damage is desirable.[15–21] We used RADAR and DDLS, both automatically calculated from ODPs by a neural network, to measure structural glaucomatous optic disc damage.

Table 5. Results of Multivariable Risk Factor Analysis for Slope of Rim Area to Disc Area Ratio

Variables	Odds Ratio	95% CI
Age	0.96	0.95–0.98
SD of IOP	0.87	0.79–0.97
Race		
Caucasian	Reference	Reference
Asian	0.42	0.25–0.69
Black or African American	0.83	0.45–1.54
Hispanic	0.61	0.31–1.20
Other	0.90	0.58–1.39
MD baseline	1.05	1.01–1.08
Diagnosis		
POAG	Reference	Reference
PACG	0.98	0.39–2.43
SOAG	0.87	0.39–1.95
GS	1.2	0.77–2.03

Table 4. Baseline RADAR and Slope of RADAR According to Type of Glaucoma

Characteristic	GS	POAG	PACG	SOAG
Number (%) of eyes	842	2971 (91.0[a])	131 (4.0[a])	164 (5.0[a])
Baseline RADAR	0.67 ± 0.13	0.57 ± 0.18	0.59 ± 0.17	0.58 ± 0.18
Slope RADAR	−0.008 ± 0.032	−0.010 ± 0.027	−0.010 ± 0.028	−0.013 ± 0.031
Baseline MD, dB	−1.36 ± 3.11	−3.38 ± 4.72	−4.4 ± 5.31	−3.76 ± 5.61
mean IOP, mm Hg	15.1 ± 3.20	14.3 ± 4.38	14.8 ± 3.02	14.5 ± 2.97
Peak IOP, mm Hg	18.8 ± 5.78	20.1 ± 7.12	21.1 ± 7.43	22.3 ± 7.26
SD of IOP, mm Hg	2.14 ± 1.35	2.7 ± 1.60	2.97 ± 2.01	3.33 ± 2.07

Values are presented as the mean ± SD unless otherwise indicated.
[a]Proportion of all glaucoma patients.

Table 6. Baseline DDLS and Slope of DDLS According to Stage of Glaucoma

Characteristic	GS	Early	Moderate	Advanced
Number (%) of eyes	842	2607 (79.9[a])	409 (12.5[a])	248 (7.6[a])
Baseline DDLS	3.78 ± 0.95	4.14 ± 1.01	5.09 ± 1.32	5.92 ± 1.62
Slope of DDLS	0.11 ± 0.28	0.11 ± 0.27	0.14 ± 0.34	0.07 ± 0.39

Values are presented as the mean ± SD unless otherwise indicated.
[a]Proportion of all glaucoma patients.

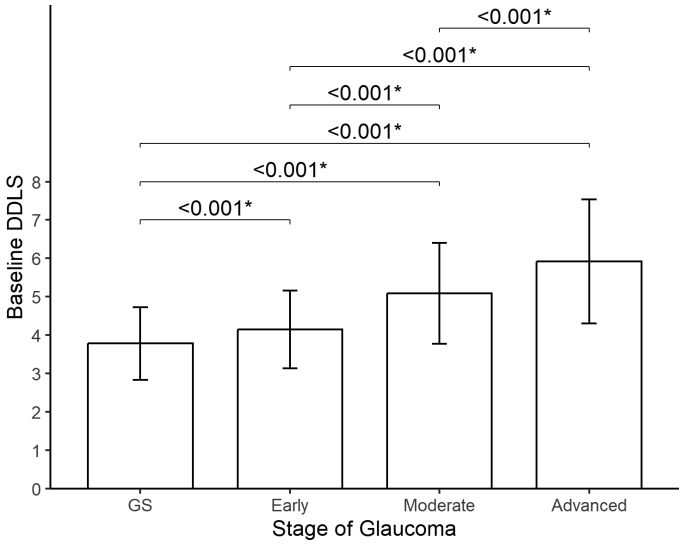

Figure 4. Comparison of baseline disc damage likelihood scale according to stage of glaucoma. Early = early-stage glaucoma; moderate = moderate-stage glaucoma; advanced = advanced-stage glaucoma. *Statistical significance by one-way analysis of variance with post hoc multiple comparison (Scheffé method).

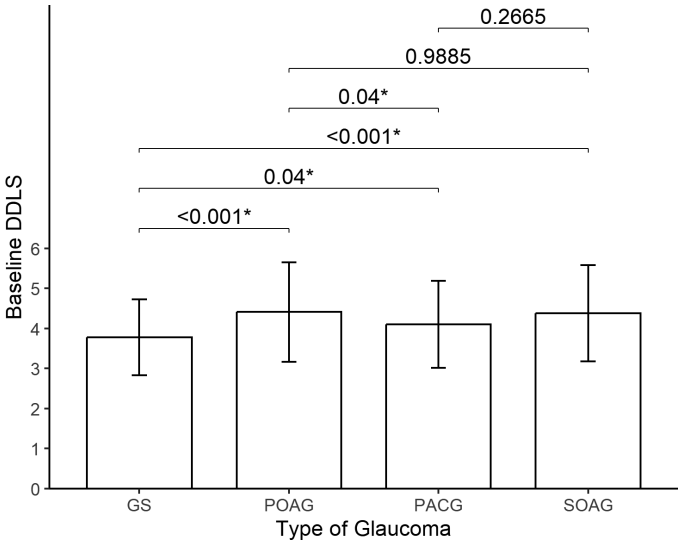

Figure 5. Comparison of baseline disc damage likelihood scale according to type of glaucoma. *Statistical significance by one-way analysis of variance with post hoc multiple comparison (Scheffé method).

We broadly evaluated longitudinal change of RADAR in glaucoma and GS patients and found that RADAR was significantly decreased after a follow-up period of approximately 5 years in glaucoma and GS patients. Previously published studies confirmed that structural changes over time are occurring in both glaucomatous and healthy eyes.[28,29] Therefore, some of this decrease in our study could be a physiologic change over time in glaucoma patients receiving treatment and in GS patients.

Several studies have reported RADAR in patients with glaucoma and GS.[24,28,29] Rolando et al.,[24] Baskaran et al.,[30] and Tezel et al.[31] reported that mean ± SD RADAR in patients with glaucoma was 0.47 ± 0.04, 0.17 ± 0.01, and 0.34 ± 0.17, respectively. In Baskaran et al.,[30] RADAR was manually calculated with data derived from Cirrus high-definition OCT and included in the analysis as a measure adjusting for variation in disc area. Tezel et al.[31] and Rolando et al.[24] used data derived from ODPs. In the present study,

Table 7. Baseline DDLS and Slope of DDLS According to Type of Glaucoma

Characteristic	GS	POAG	PACG	SOAG
Number (%) of eyes	842	2971 (91.0[a])	131 (4.0[a])	164 (5.0[a])
Baseline DDLS	3.78 ± 0.95	4.41 ± 1.24	4.10 ± 1.09	4.37 ± 1.20
Slope of DDLS	0.11 ± 0.28	0.11 ± 0.29	0.11 ± 0.27	0.12 ± 0.29

Values are presented as the mean ± SD unless otherwise indicated.
[a]Proportion of all glaucoma patients.

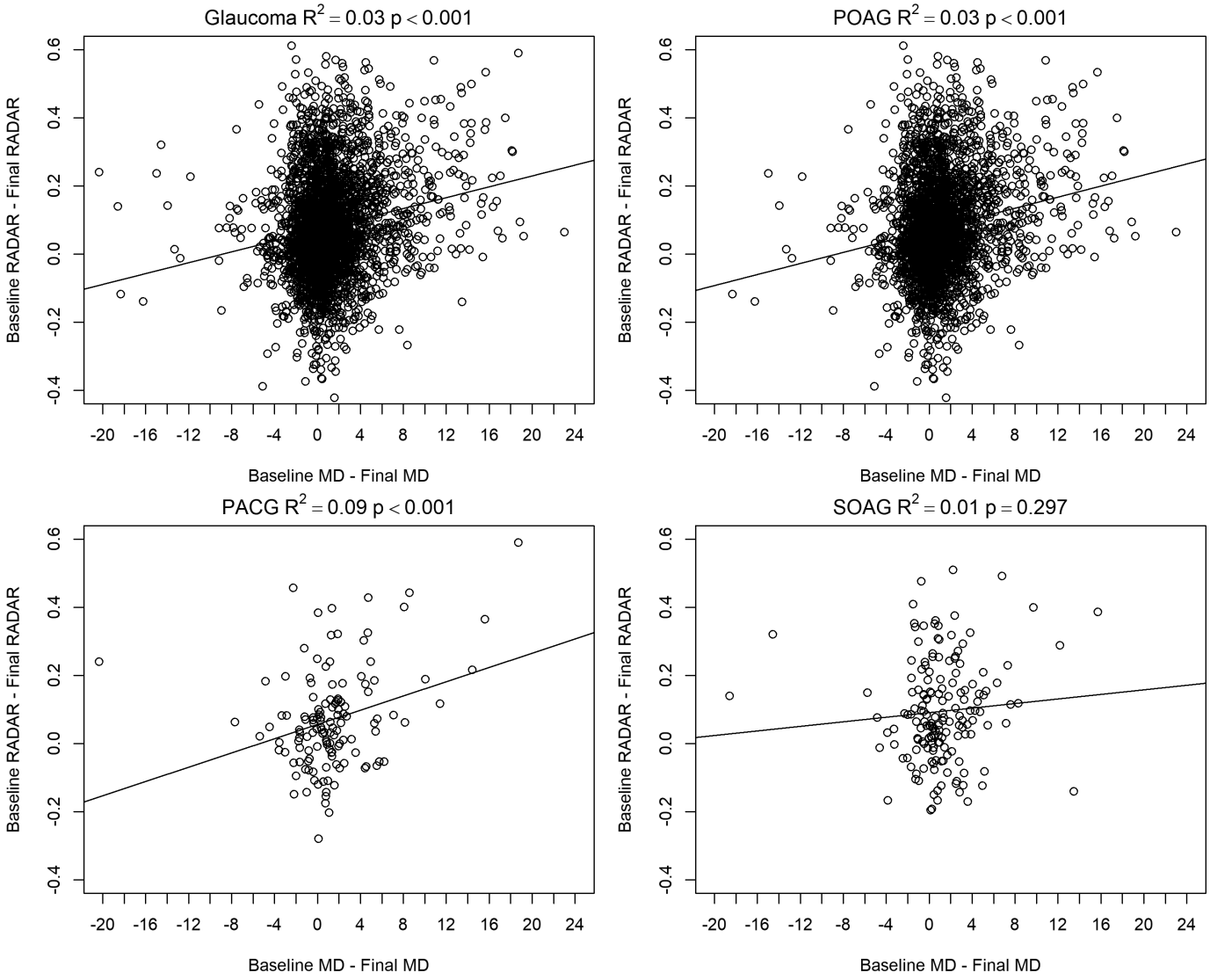

Figure 6. Correlation between difference in rim to disc area ratio and difference in mean deviation at each glaucoma group. *Statistical significance. $P < 0.05$.

the neural network–calculated mean ± SD baseline RADAR derived from ODPs in glaucoma patients was 0.57 ± 0.18. The RADAR that we reported was higher compared with previous studies.[24,30,31] This result may be due to differences in the glaucoma stage distribution among the studies. Our study included a greater portion of early-stage glaucoma (79.9%), with a baseline MD of −1.93 db. Baskaran et al.[30] and Rolando et al.[24] reported baseline MD values of −8.1 dB and −5.53 dB. This indicates a greater proportion of moderate or advanced stage of glaucoma than in our patient cohort, although they did not include a full distribution of the glaucoma stages represented in their study population. The study by Tezel et al.[31] did not provide the distribution of glaucoma stage or baseline MD.

When adjusting for MD, the baseline RADAR of POAG was significantly lower than that of PACG. No other differences between POAG, PACG, and SOAG were observed with this metric. There are no previous studies comparing RADAR in various types of glaucoma. However, several previous studies have reported certain characteristics of ONH parameters between two different subtypes of glaucoma. Sihota et al.[32] reported that chronic primary angle closure glaucoma (CPACG) eyes, in comparison to POAG eyes, had a significantly higher RADAR (CPACG RADAR: 0.56; POAG RADAR: 0.41). Nouri-Mahdavi et al.[33] also reported that CACG patients had a significantly higher RADAR than POAG patients (CACG RADAR: 0.57; POAG RADAR: 0.48). Our results, in which baseline

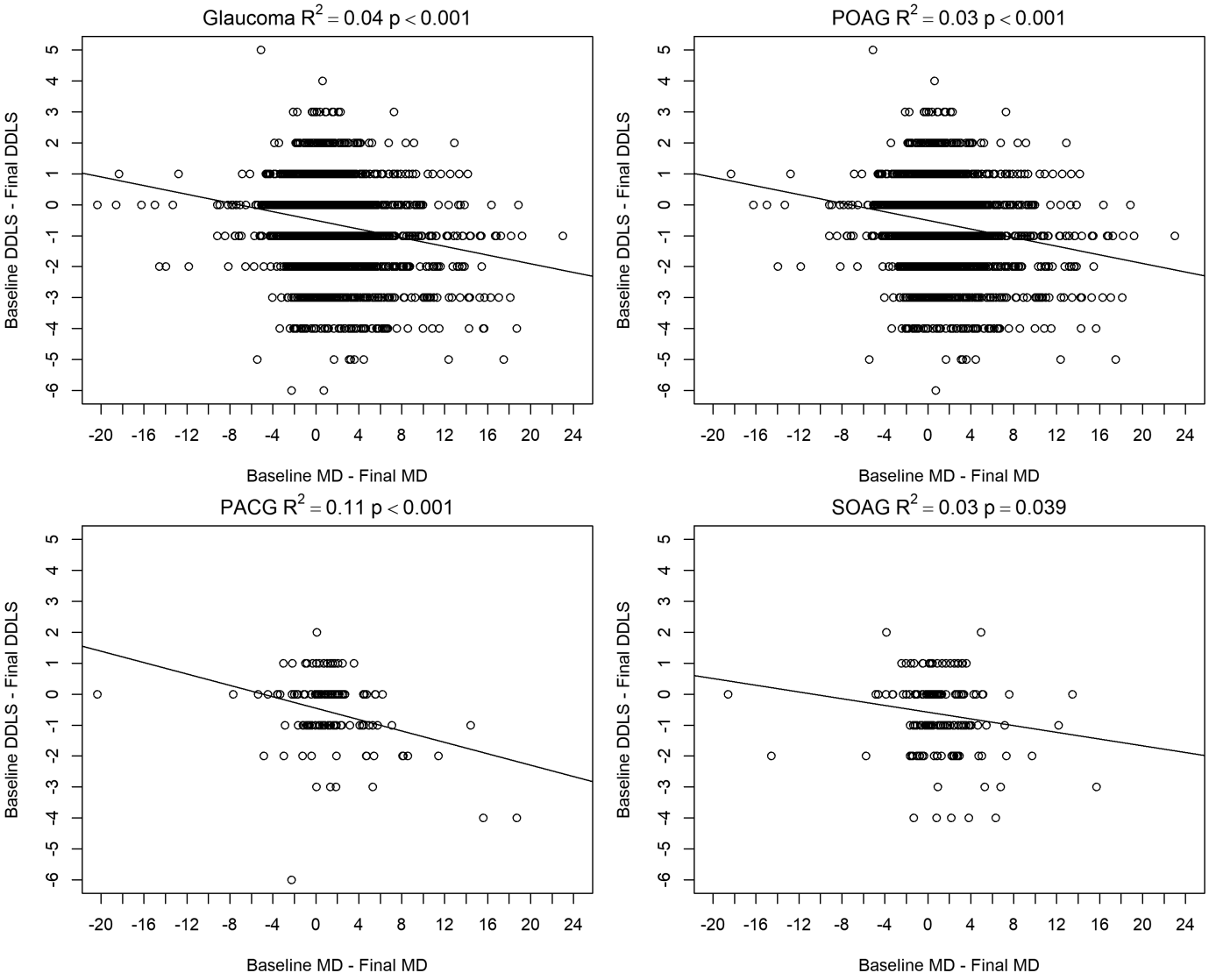

Figure 7. Correlation between difference in disc damage likelihood scale and difference in mean deviation at each glaucoma group. *Statistical significance. $P < 0.05$.

RADAR of POAG was lower than that of PACG, are consistent with the findings of these previous studies.[32,33] However, Borand et al.[34] found there are no significant differences in ONH topography between POAG and PACG. They used data including cup area, rim area, cup-to-disc area ratio, cup volume, rim volume, mean cup depth, and cup shape measure. Zhao et al.[35] reported that there was no difference in RADAR derived from Heidelberg retina tomograph (HRT) between CACG and normal-tension glaucoma (NTG) (CACG RADAR: 0.659; NTG RADAR: 0.547). This variation among previous studies and our study was also likely a product of a difference in the metrics evaluating structural glaucomatous damage and the glaucoma populations.

We also evaluated characteristics of DDLS according to stage and type of glaucoma. Abdul Majid et al.[36] reported that eyes with GS and glaucoma had mean ± SD DDLS of 5.33 ± 1.39 and 2.55 ± 1.93, respectively. In our study, the mean ± SD DDLS in GS and glaucoma patients was 3.78 ± 0.95 and 4.39 ± 1.23. In a study conducted by Kara-José et al.,[37] the median DDLS of glaucoma, including POAG and preperimetric glaucoma, was 5. Kitaoka et al.[38] reported that the mean ± SD DDLS of POAG, including NTG, was 3.77 ± 0.95. Our study found that the mean ± SD DDLS in POAG was 4.41 ± 1.24. Direct comparison between previous studies and our study is not possible because the type and stage of glaucoma differed.

In our study, both suspected and advanced glaucoma had a less steep slope of RADAR compared

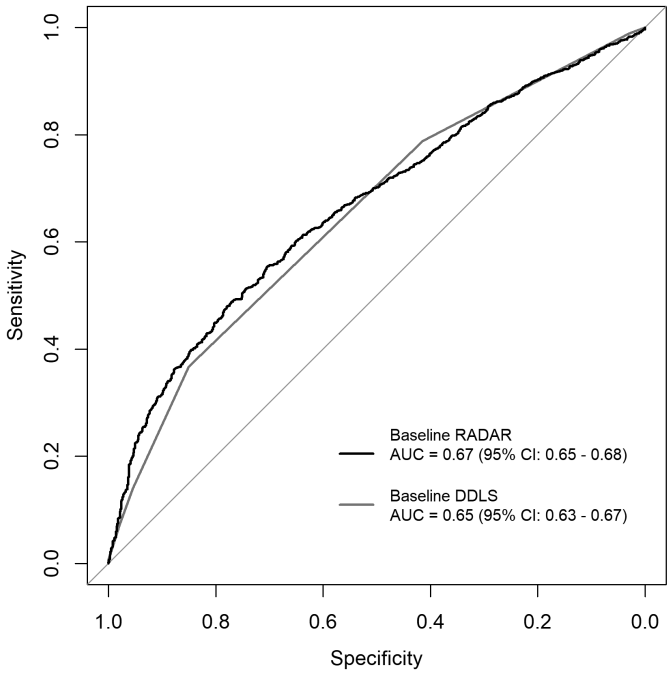

Figure 8. ROC curves of rim area to disc area ratio and disc damage likelihood scale to distinguish glaucoma suspect and glaucoma. CI, confidence interval.

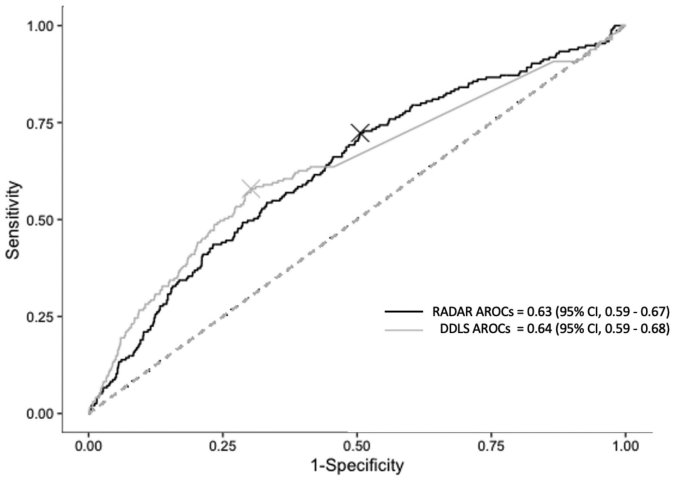

Figure 9. ROC curves of rim area to disc area ratio and disc damage likelihood scale to discriminate progression of glaucomatous visual field defect from no progression. CI, confidence interval.

to that of early or moderate glaucoma. In addition, we also found that the DDLS had a less steep slope in advanced glaucoma. There exists a floor effect for evaluating structural glaucomatous progression in advanced glaucoma; as measurements approach their floor, the apparent rate of decline diminishes.[39] Several studies reported similar results.[19,40,41] Caprioli[40] demonstrated that the ratio of the rate of structural change (measured by disc rim area) to functional change (measured by visual field–corrected loss variance) decreases as the disease progresses. Therefore, at more advanced stages, perimetric measurements may be more sensitive than optic disc evaluation to detect disease progression. Zeyen et al.and Caprioli[41] demonstrated that the ratio of disc change to visual field change is low in more advanced glaucoma, which supports this conclusion. Danesh-Meyer et al.[19] similarly showed that advanced stages of structural glaucomatous change were associated with minimal visual field change. Our results, in which RADAR and DDLS both demonstrated slower progression in advanced glaucoma, are consistent with a floor effect and the findings of these previous studies.

Our results showed that a diagnosis of SOAG is also a risk factor for glaucoma progression. In our study population, the SOAG subgroup was predominantly composed of exfoliation glaucoma. Several studies have shown that exfoliation glaucoma runs a more aggressive and severe course than other types of glaucoma.[42–44] In addition, SOAG patients tend to have higher peak IOPs and greater IOP fluctuations as compared to patients with GS, POAG, and PACG and therefore are predisposed to progression of RADAR.

Our study also examined the correlation between the difference in both RADAR and DDLS and that of MD. We found that changes in both metrics were positively correlated with changes in MD in glaucoma patients. There was also a significant correlation between RADAR and MD in each analyzed subtype of glaucoma, confirming that this metric reflected the change of MD in POAG, PACG, and SOAG. However, the correlation coefficient between the difference in both RADAR and DDLS and that of MD was low. This is thought to be because structural and functional changes in glaucoma differ in the timing and degree of occurrence. Despite a low correlation coefficient, this study demonstrates the value to determine whether glaucoma progresses with deep neural network–generated RADAR and DDLS, which both represent structural glaucomatous damage.

We compared RADAR and DDLS in their utility in distinguishing glaucoma from GS and detecting glaucoma progression. There have been several studies comparing DDLS and CDR in both tasks. Philippin et al.[45] reported that both DDLS and CDR can differentiate severe glaucoma from less severe disease, with a moderate advantage of DDLS over CDR. Kara-José et al.[37] reported that DDLS and CDR demonstrated excellent accuracy in distinguishing glaucomatous from healthy eyes. However, there were no previous studies on the ability of RADAR or DDLS to distinguish glaucoma from GS. In our study, we confirmed that RADAR and DDLS had similar

diagnostic abilities to discriminate glaucoma from GS and to detect glaucoma progression. Therefore, our results are relevant since it is the first study to confirm the ability of RADAR and DDLS, measured with machine learning techniques, to distinguish glaucoma from GS despite their low AUC.

Our study is not without limitations. First, the retrospective design involved a tertiary care setting that may have introduced selection bias. Second, we defined functional glaucomatous damage with MD and compared this metric to RADAR or DDLS for evaluation of correlation; we did not use any other parameter or methods to assess functional glaucomatous damage. Third, we could not determine whether the change in RADAR over time was entirely due to the progression of glaucoma because there are no predefined criteria for age-related changes of RADAR. Fourth, our study population had a high proportion of early-stage glaucoma eyes compared to the proportion of moderate or advanced glaucoma eyes. Fifth, our results did not reflect aging changes of RADAR and DDLS. To the best of our knowledge, this is the first study reporting large population-based data of baseline and longitudinal change of artificial intelligence–derived RADAR and DDLS based on ODPs according to type and stage of glaucoma.

In conclusion, our study provides large-scale data for RADAR and DDLS in glaucoma and GS patients calculated with artificial intelligence. The differences in RADAR and DDLS were both weakly but statistically significantly correlated with a corresponding change in MD. RADAR and DDLS had similar diagnostic abilities to discriminate glaucoma from GS and to detect glaucoma progression. This demonstrates that automated segmentation of ODPs and calculation of RADAR and DDLS with a neural network can be used to evaluate the extent and long-term rate of optic disc rim loss and is further evidence of long-term nerve fiber loss in patients treated for glaucoma.

Acknowledgments

Supported by grants from the Simms/Mann Family Foundation, the Payden Memorial Foundation, and Research to Prevent Blindness (JC). The funders had no role in the design and conduct of the study; collection, management, analysis, and interpretation of the data; preparation, review, or approval of the manuscript; and decision to submit the manuscript for publication.

Disclosure: **S.W. Jin**, None; **E. Bouris**, None; **E. Morales**, None; **J. Caprioli**, None

References

1. Van Buskirk EM, Cioffi GA. Glaucomatous optic neuropathy. *Am J Ophthalmol*. 1992;113:447–452.
2. Sommer A, Katz J, Quigley HA, et al. Clinically detectable nerve fiber atrophy precedes the onset of glaucomatous field loss. *Arch Ophthalmol*. 1991;109:77–83.
3. Tuulonen A, Airaksinen PJ. Initial glaucomatous optic disk and retinal nerve fiber layer abnormalities and their progression. *Am J Ophthalmol*. 1991;111:485–490.
4. Caprioli J. The importance of rates in glaucoma. *Am J Ophthalmol*. 2008;145:191–192.
5. Giaconi JA, Law SK, Coleman AL, Caprioli J. *Pearls of Glaucoma Management*. Berlin: Springer; 2010.
6. Jampel HD, Friedman D, Quigley H, et al. Agreement among glaucoma specialists in assessing progressive disc changes from photographs in open-angle glaucoma patients. *Am J Ophthalmol*. 2009;147:39–44.e1.
7. Lee T, Jammal AA, Mariottoni EB, Medeiros FA. Predicting glaucoma development with longitudinal deep learning predictions from fundus photographs. *Am J Ophthalmol*. 2021;225:86–94.
8. Hoffmann EM. Optic disc photography and retinal nerve fiber layer photography. *Ophthalmologe*. 2009;106:683–686.
9. Abrams LS, Scott IU, Spaeth GL, Quigley HA, Varma R. Agreement among optometrists, ophthalmologists, and residents in evaluating the optic disc for glaucoma. *Ophthalmology*. 1994;101:1662–1667.
10. Armaly MF. Genetic determination of cup/disc ratio of the optic nerve. *Arch Ophthalmol*. 1967;78:35–43.
11. Gordon MO, Beiser JA, Brandt JD, et al. The ocular hypertension treatment study: baseline factors that predict the onset of primary open-angle glaucoma. *Arch Ophthalmol*. 2002;120:714–720.
12. Gulshan V, Peng L, Coram M, et al. Development and validation of a deep learning algorithm for detection of diabetic retinopathy in retinal fundus photographs. *JAMA*. 2016;316:2402–2410.
13. Bartz-Schmidt KU, Weber J, Heimann K. Validity of two-dimensional data obtained with the Heidelberg retina tomograph as verified by direct mea-

surements in normal optic nerve heads. *Ger J Ophthalmol*. 1994;3:400–405.
14. Jonas JB, Zäch FM, Gusek GC, et al. Pseudoglaucomatous physiologic large cups. *Am J Ophthalmol*. 1989;107:137–144.
15. Carpel EF, Engstrom PF. The normal cup-disk ratio. *Am J Ophthalmol*. 1981;91:588–597.
16. Jonas JB, Budde WM, Panda-Jonas S. Ophthalmoscopic evaluation of the optic nerve head. *Surv Ophthalmol*. 1999;43:293–320.
17. Bayer A, Harasymowycz P, Henderer JD, Steinmann WG, Spaeth GL. Validity of a new disc grading scale for estimating glaucomatous damage: correlation with visual field damage. *Am J Ophthalmol*. 2002;133:758–763.
18. Spaeth GL, Henderer J, Liu C, et al. The disc damage likelihood scale: reproducibility of a new method of estimating the amount of optic nerve damage caused by glaucoma. *Trans Am Ophthalmol Soc*. 2002;100:181–185.
19. Danesh-Meyer HV, Gaskin BJ, Jayusundera T, Donaldson M, Gamble GD. Comparison of disc damage likelihood scale, cup to disc ratio, and Heidelberg retina tomograph in the diagnosis of glaucoma. *Br J Ophthalmol*. 2006;90:437–441.
20. Rasheed HA, Davis T, Morales E, et al. DDLSNet: a novel deep learning-based system for grading funduscopic images for glaucomatous damage. *Ophthalmol Sci*. 2022;3:100255.
21. Rasheed HA, Davis T, Morales E, et al. RimNet: a deep neural network pipeline for automated identification of the optic disc rim. *Ophthalmol Sci*. 2022;3:100244.
22. Klein B, Magli Y, Richie K, Moss S, Meuer S, Klein R. Quantification of optic disc cupping. *Ophthalmology*. 1985;92:1654–1656.
23. Bartz-Schmidt KU, Sengersdorf A, Esser P, Walter P, Hilgers RD, Krieglstein GK. The cumulative normalised rim/disc area ratio curve. *Graefes Arch Clin Exp Ophthalmol*. 1996;234:227–231.
24. Rolando M, Macrì A, Iester M, Altieri M, Calabria G. RA/DA cumulative curve analysis of local and diffuse neuroretinal rim area damage in glaucoma patients. *Br J Ophthalmol*. 1998;82:769–772.
25. Rabiolo A, Morales E, Mohamed L, et al. Comparison of methods to detect and measure glaucomatous visual field progression. *Transl Vis Sci Technol*. 2019;8:2.
26. Anderson DR, Patella VM. *Automated Static Perimetry*. 2nd ed. St. Louis, MO: Mosby; 1999:121–190.
27. Medeiros FA, Zangwill LM, Bowd C, Mansouri K, Weinreb RN. The structure and function relationship in glaucoma: implications for detection of progression and measurement of rates of change. *Invest Ophthalmol Vis Sci*. 2012;53:6939–6946.
28. Hammel N, Belghith A, Bowd C, et al. Rate and pattern of rim area loss in healthy and progressing glaucoma eyes. *Ophthalmology*. 2016;123:760–770.
29. Patel NB, Gajjar A, Evans KB, Harwerth RS. Age-associated changes in the retinal nerve fiber layer and optic nerve head. *Invest Ophthalmol Vis Sci*. 2014;55:5134–5143.
30. Baskaran M, Ong EL, Li JL, et al. Classification algorithms enhance the discrimination of glaucoma from normal eyes using high-definition optical coherence tomography. *Invest Ophthalmol Vis Sci*. 2012;53:2314–2320.
31. Tezel G, Siegmund KD, Trinkaus K, Wax MB, Kass MA, Kolker AE. Clinical factors associated with progression of glaucomatous optic disc damage in treated patients. *Arch Ophthalmol*. 2001;119:813–818.
32. Sihota R, Saxena R, Taneja N, Venkatesh P, Sinha A. Topography and fluorescein angiography of the optic nerve head in primary open-angle and chronic primary angle closure glaucoma. *Optom Vis Sci*. 2006; 83:520–526.
33. Nouri-Mahdavi K, Supawavej C, Bitrian E, et al. Patterns of damage in chronic angle-closure glaucoma compared to primary open-angle glaucoma. *Am J Ophthalmol*. 2011;152:74–80.e2.
34. Boland MV, Zhang L, Broman AT, et al. Comparison of optic nerve head topography and visual field in eyes with open-angle and angle-closure glaucoma. *Ophthalmology*. 2008; 115:239–245.e2.
35. Zhao L, Wu L, Wang X. Optic nerve head morphologic characteristics in chronic angle-closure glaucoma and normal-tension glaucoma. *J Glaucoma*. 2009;18:460–463.
36. Abdul Majid AS, Kwag JH, Jung SH, Yim HB, Kim YD, Kang KD. Correlation between disc damage likelihood scale and optical coherence tomography in the diagnosis of glaucoma. *Ophthalmologica*. 2010;224:274–282.
37. Kara-José AC, Melo LAS, Jr, Esporcatte BLB, Endo ATNH, Leite MT, Tavares IM. The disc damage likelihood scale: diagnostic accuracy and correlations with cup-to-disc ratio, structural tests and standard automated perimetry. *PLoS One*. 2017;12:e0181428.
38. Kitaoka Y, Tanito M, Yokoyama Y, et al. Estimation of the Disc Damage Likelihood Scale in primary open-angle glaucoma: the Glaucoma Stereo Analysis Study. *Graefes Arch Clin Exp Ophthalmol*. 2016;254:523–528.

39. Bowd C, Zangwill LM, Weinreb RN, Medeiros FA, Belghith A. Estimating optical coherence tomography structural measurement floors to improve detection of progression in advanced glaucoma. *Am J Ophthalmol*. 2017;175:37–44.
40. Caprioli J. Clinical evaluation of the optic nerve in glaucoma. *Trans Am Ophthalmol Soc*. 1994;92:589–641.
41. Zeyen TG, Caprioli J. Progression of disc and field damage in early glaucoma. *Arch Ophthalmol*. 1993;111:62–65.
42. Konstas AG, Hollo G, Astakhov YS, et al. Factors associated with long-term progression or stability in exfoliation glaucoma. *Arch Ophthalmol*. 2004;122:29–33.
43. Chan TCW, Bala C, Siu A, Wan F, White A. Risk factors for rapid glaucoma disease progression. *Am J Ophthalmol*. 2017;180:151–157.
44. Lee WJ, Baek SU, Kim YK, Park KH, Jeoung JW. Rates of ganglion cell-inner plexiform layer thinning in normal, open-angle glaucoma and pseudoexfoliation glaucoma eyes: a trend-based analysis. *Invest Ophthalmol Vis Sci*. 2019;60:599–604.
45. Philippin H, Matayan EN, Knoll KM, et al. Differentiating stages of functional vision loss from glaucoma using the Disc Damage Likelihood Scale and cup:disc ratio. *Br J Ophthalmol*. 2024;108(3):349–356.